Polynomial-based optical true-time delay devices with microelectromechanical mirror arrays

Betty Lise Anderson and Rashmi Mital

We previously reported optical true-time delay devices, based on the White cell, to support phased-array radars. In particular, we demonstrated a quadratic device, in which the number of delays obtainable was proportional to the square of the number of times the light beam bounced in the cell. Here we consider the possibilities when a microelectromechanical (MEM) tip/tilt mirror array with multiple stable states is used. We present and compare designs for quadratic, quartic, and octic cells using MEM mirror arrays with two, three, and five micro-mirror tilt angles. An octic cell with a three-state MEM can produce 6,339 different delays in just 17 bounces. © 2002 Optical Society of America

OCIS codes: 230.6120, 160.3710, 070.1170.

1. Introduction

This work was motivated by the desire to provide true-time delays (TTD)s for phased-array radars. Phased arrays possess many antenna elements, whose individual beams combine to produce a single, well-shaped and highly directional radar beam. By varying the timing of the arrival of the rf signals at the elements, the radar beam can be steered electronically.[1]

In optical TTD, the rf signals are modulated onto light beams, and then the light beams are delayed for varying amounts of time. Many examples exist in the literature.[2–9] The term true time distinguishes this approach from simpler techniques that use only phase shifters. Phase shifting, however, works well only near a single frequency and produces beam squint in broadband antennas.[1]

Producing optical delays has other uses, as well. For example, by using an optical tapped delay line, one can produce a pulse stream from a single laser pulse,[10,11] or compress or decompress a data rate.[10] Tapped delay lines can be used in optical computing.[12,13] By adding appropriate weights at each tap, one can produce a transversal adaptive filter.[10,14–16] Using such a filter in an optical correlator/decorrelator, one can provide an implementation for encoding and decoding addresses in optical code division multiplexing.[17]

Our approach to optical TTD is a free-space device based on the White cell. Our White-cell-based TTD designs can be generally divided into two classes. One is a class of polynomial cells in which the number of delays N is proportional to some power of the number of bounces m a light beam makes off the microelectromechanical (MEM) mirror arrays. For example, a quadratic cell would provide $N \propto m^2$.[18,19] The other is a class of exponential cells in which the number of delays is proportional to some number raised to the power of the number of bounces. An example is a binary cell, in which $N \propto 2^m$ (we intend to report on this separately). Most previous work in optical TTD produces devices that are binary in the number of times the beam is optically switched, for example.[9,20,21] Polynomial approaches are usually[22,23] but not always[24] linear (the number of delays is proportional to the number of switches or sources).

We built and demonstrated a quadratic TTD device based on the White cell and using a liquid-crystal spatial light modulator (SLM).[25] The number of delays produced was proportional to m^2, where m is the number of bounces. We built and demonstrated a linear cell (the simplest of the polynomial cells) that used a two-state MEM, specifically the Texas Instruments (TI) digital micromirror device (DMD®). This TI device produced a number of delays that was directly proportional to the number of bounces.

Here our intention is to explore higher-order polynomial TTD devices. We start with a quadratic cell

The authors are with the Department of Electrical Engineering, The Ohio State University, 205 Dreese Laboratory, 2015 Neil Avenue, Columbus, Ohio 43210. B. L. Anderson's e-mail address is anderson@ee.eng.ohio-state.edu.

Received 6 March 2002; revised manuscript received 8 May 2002.

0003-6935/02/265449-13$15.00/0

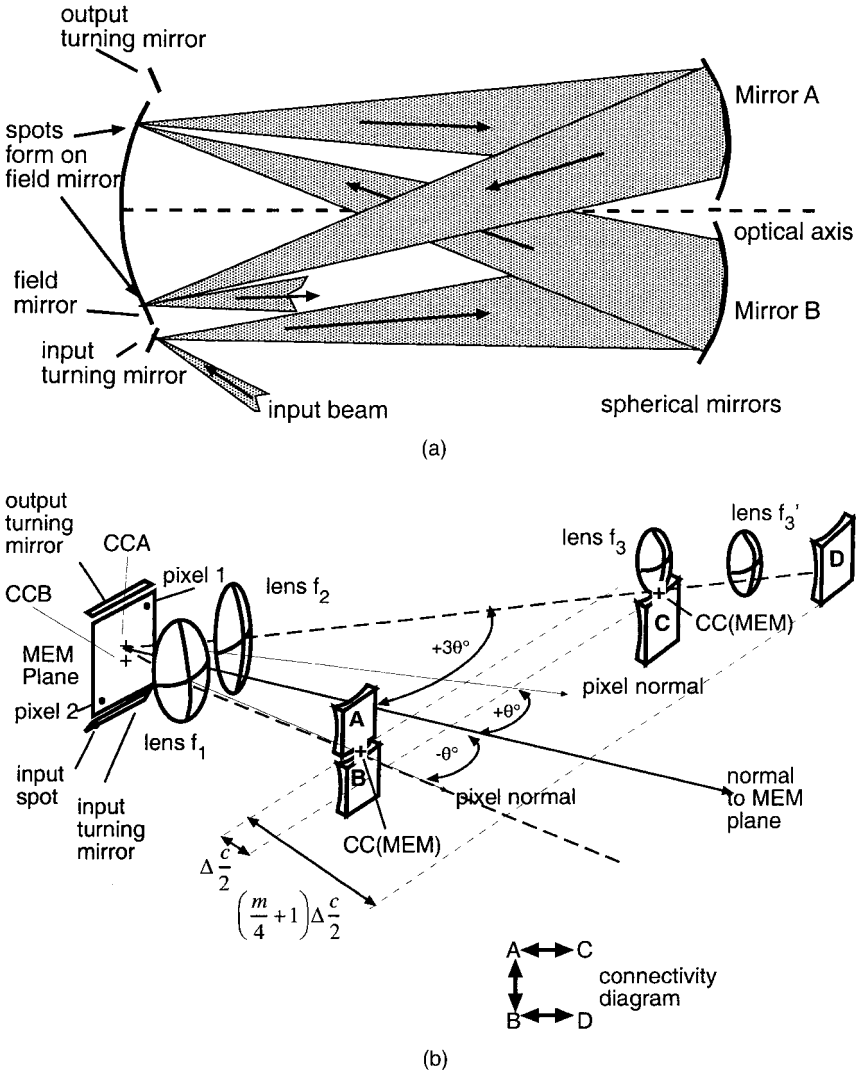

Fig. 1. (a) Original White cell. Beams bounce multiple times between a set of three spherical mirrors, tracing out a pattern of spots on the left-hand-side mirror. (b) Quadratic optical TTD device with a MEM in place of the left-hand-side White-cell mirror. White cells have been set up along two axes, one at $-\theta$ and one at $+3\theta$, where the MEM here is assumed to have two stable states, tipping to plus or minus θ.

based on a two-state MEM like the TI DMD®. We then extend our ideas to hypothetical MEM mirror arrays having three or more stable states. These are termed digital in the sense that the number of MEM states is finite and discrete. The micromirrors of analog MEM mirror arrays, however, can tilt to any arbitrary angle within some range. These provide in theory an unlimited number of states and thus a TTD cell of very-high capability. We show that in practice such a capable but complex MEM is probably not needed for polynomial TTDs.

We begin by reviewing the quadratic cell briefly in Section 2, and in the process summarize the operation of a White cell and the significance of the spot patterns. In Section 3 we propose a quartic cell in which the number of delays is proportional to m^4. This design uses a MEM with three stable states. In Section 4 we investigate even higher-order designs based on MEM mirror arrays having more than two stable states. We provide some discussion and conclusions in Section 5.

2. Quadratic Cell with Two-State Microelectromechanical Mirror Arrays and Multiple White Cells

Our optical TTD devices are all based on the White cell, a system of three spherical mirrors of identical radii of curvature.[26] Figure 1(a) shows that a beam is introduced into the cell, by way of a spot on an input turning mirror, and bounces back and forth between the mirrors. The light is reflected to a new spot on each bounce. A pattern of spots forms on one of the mirrors (the field mirror), and the locations of the spots for a given light beam are determined by the alignment of the other two mirrors (A and B). Only the first couple of bounces are shown, but eventually the spots will cease to fall on the mirror on the left

and be directed out of the cell by an output turning mirror.

We described how to adapt the White cell to TTD in some detail previously,[27] so here we present only a short review. First, we replace the mirror on the left of Fig. 1(a) with a reflecting spatial light modulator (SLM) and a lens. This SLM/lens combination reproduces the reflecting and focusing function of the original spherical mirror. Let us take the SLM to be a MEM device with tilting micromirrors, and let us assume the mirror can tip to one of two stable positions at $\pm\theta$ with respect to the MEM normal. An example of such a device would be the TI DMD®.

Figure 1(b) shows that because the MEM has two stable states, we can construct White cells in two directions. Thus there are two field lenses f_1 and f_2 in front of the MEM. On an axis at $-\theta$ to the normal to the MEM plane, mirrors A and B form a White cell with the MEM and lens f_1. That is, if the micromirrors are all tipped to $-\theta$, then light coming from A will form a spot on the MEM, and be directed to B, and light coming from B will be similarly returned to A. A spot pattern will form on the MEM with each spot striking a different pixel.

If, however, light coming from A forms a spot on a pixel that is being tilted to $+\theta$, the light is reflected in a direction at $+3\theta$ with respect to the MEM plane normal. We place two more spherical mirrors along this axis. For example, light coming from A in this case goes to mirror C and from C back to A. Thus A and C form a White cell with the MEM. Mirror C, however, is placed at a slightly greater distance from the MEM (thus $f_1 \neq f_2$), which introduces a time delay for a beam sent to C. If we call our minimum time-delay increment Δ, then the distance to C is $\Delta c/2$ further from the MEM than mirror A.

Similarly, if light is coming from mirror B, and the micromirror is tipped to $+\theta$, then the light will go to D. Thus B and D also form a White cell. We choose mirror D to be further from the MEM by a distance $(m/4 + 1)\Delta c/2$, as discussed later. Extra lenses are added to the arm containing mirror D to fulfill the imaging requirements of the White cell.

The connectivity diagram in Fig. 1(b) shows the possible transitions by use of this MEM device.

Let us next examine the spot pattern that forms on the MEM. A beam is input into the cell as a spot formed on the input turning mirror. Suppose the input turning mirror is tipped so that the light is directed to mirror B. Mirror B reflects the input spot onto the MEM, the image forming at spot No. 1. This construction is shown in Fig. 2. The position of this spot is determined by the location of the center of the curvature of mirror B (or more accurately, the location of the image of the center of curvature of mirror B [CC(B)] on the MEM plane). Let us assume the micromirror at that pixel is tipped to $-\theta$. Light is therefore reflected back into the AB White cell.

If the field lens f_1 and the MEM are considered as jointly replacing a spherical mirror, then the effective center of curvature of this mirror [CC(MEM)] is

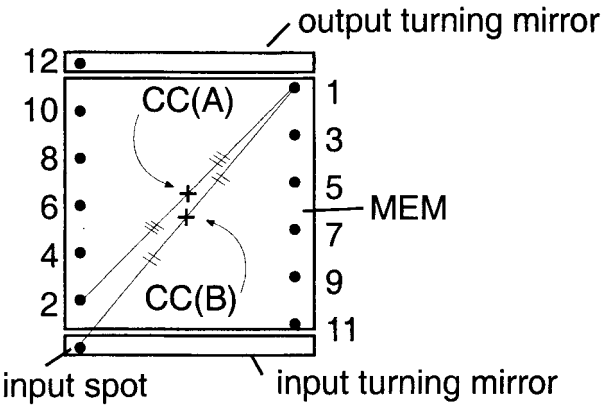

Fig. 2. Spot patterns produced for a single input beam in a White cell.

placed between mirrors A and B when the pixels are tipped to $-\theta$. Thus the light from mirror B is reflected onto mirror A. This is a key feature of the White cell. Because the spots on the MEM will be small, the beams will diverge significantly. That does not matter, however, because the diverging beam will still fit onto mirror B, and that light will reappear at mirror A. Thus there are no diffraction losses.

Let us return to the progression of spots. So far we had light entering by way of the input turning mirror, going to mirror B, forming a new spot and then diverging on its way to mirror A. Now, mirror A treats spot No. 1 as an object, and refocuses the beam to a new image on the MEM, at spot No. 2, located at an equal and opposite distance on the opposite side of mirror A's center of curvature. Spot 2 is an object for mirror B, which reflects it again to the next location on the MEM. The spot process continues, producing a set of spots on the MEM as shown in Fig. 2. Even-numbered bounces form a column going upward on one side of the MEM and the odd-numbered spots form a second column, progressing downward. The spacing between the spots is determined entirely by the alignment of the centers of curvature of the two mirrors A and B.

Next, suppose that on the second bounce the MEM pixel is tipped to $+\theta$ instead of $-\theta$. Then light arriving at that pixel from mirror A is sent to mirror C instead of B. Mirror C is placed slightly farther from the MEM than A and B, so that light going there takes some time Δ longer to return to the MEM. Mirror C is aligned in such a way that its center of curvature CC(C) is co-located with CC(B), so that whether the light goes to B or to C, it is reflected to the next spot in the same place (spot 2 in this case); only the propagation time is different. When the light returns from mirror C, the next pixel (the second bounce) must also be sent to $+\theta$ to return the beam to the AB White cell.

Similarly, if light is coming from mirror B, and the MEM pixel is tipped to $+\theta$, the beam will go to mirror D. Mirror D is placed some distance further from the MEM to produce a longer time delay. The (im-

age of the) center of curvature of mirror D is co-aligned with that of mirror A on the MEM. Thus the input beam in Fig. 2 will trace out the same spot pattern regardless of how many times it is sent to A, B, C, or D.

We observe that light must always go from an upper mirror (A or D) to a lower mirror (B or C). Further, the total number of bounces a beam makes is fixed: determined by the locations of the centers of curvature of the spherical mirrors and the overall size of the MEM.

Let the number of bounces be m. The beam will travel to the upper mirrors $m/2$ times and lower mirrors $m/2$ times.

Suppose the beam is sent to A and B on every bounce. This is the shortest possible path through the White-cell device, and the beam must always travel at least this far, and thus always have at least this minimum delay. We call AB the null cell, and the delay incurred in it is in effect subtracted out.

Next, suppose the beam is sent to mirror C one time. It incurs an extra time delay of Δ. If the beam is sent to C twice, it gets delayed by 2Δ and so forth. The maximum number of times the beam can go to mirror C is $m/2$ times for a net delay of $(m/2)\Delta$.

Thus it would seem that we should choose mirror D to be placed so that the time to it (and back) is one time-delay increment greater than this maximum to obtain the next number in the sequence. This is, however, not the case. It is not possible for light to go directly from C to D, as shown in the connectivity diagram included in Fig. 1(b). That is because the MEM mirror has only two states: $+\theta$ will return the light beam from mirror C to mirror A, and $-\theta$ will send the beam off in a direction not being used here (-5Δ). Stated another way, if the light goes to mirror C $m/2$ times, there are no possibilities to travel to D at all. Every trip to C must be followed by a return to the AB White cell. This is different than the case for the liquid-crystal-based TTD cell in which the connectivity diagram is closed (transition from C directly to D is possible).[25]

To obtain the maximum number of delays from the MEM-based device, we allow the beam to go to mirror C a maximum of $m/4$ times, for a maximum delay of $(m/4)\Delta$. We then place mirror D so that the time required to go to it and back is one time-increment longer than this maximum. Every trip to the D arm of the cell produces a net delay of $(m/4 + 1)\Delta$. Mirror D can also be traveled to up to $m/4$ times.

The maximum net time delay T that can be produced in m bounces in this scheme is given by $m/4$ trips to D and $m/4$ trip to C:

$$T = N\Delta = \left(\frac{m}{4}\right)\left(\frac{m}{4} + 1\right)\Delta + \left(\frac{m}{4}\right)\Delta = \left[\left(\frac{m}{4}\right)^2 + 2\left(\frac{m}{4}\right)\right]\Delta, \quad (1)$$

where N is the number of delays obtainable and Δ is the basic time-delay increment. In effect we are counting in a base-$(m/4)$ system. If we go to C i times and to D j times, then i is the digit in the one's place, and j the digit in the $m/4$'s place: the next significant digit.

We can actually make a slight improvement. It is possible to go to D one extra time and as a result travel to mirror C one time fewer than $m/4$. This results in the maximum number of delays:

$$T_{\text{max,quadratic}} = \left(\frac{m}{4} + 1\right)\left(\frac{m}{4} + 1\right)\Delta + \left(\frac{m}{4} - 1\right)(1)\Delta = \left[\left(\frac{m}{4}\right)^2 + 3\left(\frac{m}{4}\right)\right]\Delta. \quad (2)$$

This device is quadratic, and can produce any integer as a multiple of delay increment Δ from 0 to N. It is quadratic in $m/4$. In 16 bounces, it would produce 24 different time delays using Eq. (1), and 28 different time delays with Eq. (2). If the connectivity diagram of Fig. 1 were a closed loop, e.g., transitions from D directly to C were also allowed (as is the case in a quadratic cell using a liquid-crystal SLM, for example[18]), then the device would be quadratic in $m/2$ (e.g., 80 delays in 16 bounces). Typical phased-array radars required hundreds or even thousands of time delays, however, so a quadratic cell is not sufficient. In the next section we explore a quartic cell, which can produce more delays for the same number of bounces.

3. Quartic Cell with a Three-State Microelectromechanical Mirror Array

A. Design with One Transitional Bounce

Next, let us suppose the MEM micromirrors have three stable tilt angles. For the sake of the argument, let them be $-\theta$, flat, and $+\theta$, as in devices reported recently.[28] Now we can add another pair of spherical White-cell mirrors E and F as shown in Fig. 3. Mirrors A and B (the null cell) are placed above and below the normal to the MEM plane, D and C are placed above and below an axis oriented at $+2\theta°$ to the MEM plane, and E and F are above and below an axis at $-2\theta°$. All of the upper mirrors have their centers of curvature in one location, and all of the lower mirrors are co-aligned with their centers of curvature at another location.

Mirrors A and B form a null cell as before. In this arrangement, when the pixels are flat, light bounces back and forth in the AB White cell. Light returning from A can also be directed to mirror C (pixel at $+\theta$), or mirror F (pixel at $-\theta$). Light returning from D can be sent next to B ($+\theta$), or to mirror F (pixel flat). The complete connectivity diagram is shown in Fig. 3. What is significant in the connectivity diagram is that there are two closed loops rather than an open loop as in the quadratic cell. Thus one of the loops (e.g., A–C–E–B) can make a quadratic cell as in Section 2, but this time quadratic in $m/2$ rather than $m/4$. The difference is that transitions directly between the two delay arms are now possible. To go from the ACEB loop to the AFDB loop requires passage through either A or B,

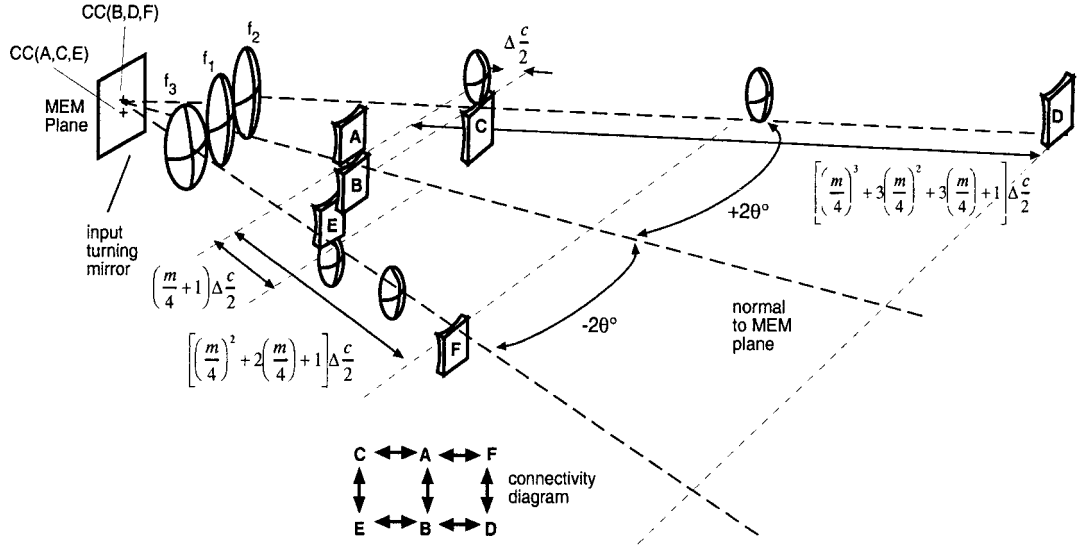

Fig. 3. Quartic cell designed around a MEM with three stable mirror states.

however. We enable one extra bounce to achieve this transition, and m is an odd number.

We therefore assign half of our remaining $m - 1$ bounces to let light circulate in the ACEB loop (the other half of the bounces are saved for the other loop). We make the transit time to C longer than to A or B by the time delay increment Δ as before. Because one quarter of the $m - 1$ bounces can go to C and another quarter to E, we make the transit time to E and back longer by $[(m - 1)/4 + 1]\Delta$, similarly to the quadratic cell. (This does not match the labeling in Fig. 3; the difference is explained in Subsection 3.B. The total number of delays using half the total bounces and just the AECB loop [compare to Equation (1)] is given by

$$N_{\mathrm{AECB}} = \left[\left(\frac{m-1}{4}\right)^2 + 2\left(\frac{m-1}{4}\right)\right]. \tag{3}$$

We next assign the delays in the other loop. We choose mirror F to be one time-delay increment longer than Eq. (3), or the length of a round trip to

$$\begin{aligned} \mathrm{F} \Rightarrow & \left[\left(\frac{m-1}{4}\right)^2 + 2\left(\frac{m-1}{4}\right) + 1\right]\Delta \\ & = \left[\left(\frac{m-1}{4}\right) + 1\right]^2 \end{aligned} \tag{4}$$

is longer than to A or B.

We can visit this mirror up to $(m - 1/4$ times as well, producing a delay (using C, E, and F only) of

$$\begin{aligned} N_{\mathrm{F,E,C\ only}} &= \Bigg\{\underbrace{\left(\frac{m-1}{4}\right)}_{\text{trips to F}}\Bigg[\underbrace{\left(\frac{m-1}{4}\right)^2 + 2\left(\frac{m-1}{4}\right) + 1}_{\text{delay of F}}\Bigg] + \underbrace{\left(\frac{m-1}{4}\right)}_{\substack{\text{trips}\\ \text{to E}}}\Bigg[\underbrace{\left(\frac{m-1}{4}\right) + 1}_{\text{delay of E}}\Bigg] + \underbrace{\left(\frac{m-1}{4}\right)}_{\substack{\text{trips}\\ \text{to C}}}\underbrace{[1]}_{\substack{\text{delay}\\ \text{of C}}}\Bigg\} \\ &= \left[\left(\frac{m-1}{4}\right)^3 + 3\left(\frac{m-1}{4}\right)^2 + 3\left(\frac{m-1}{4}\right)\right]. \end{aligned} \tag{5}$$

We make the remaining arm D longer than this one, so that

$$\begin{aligned} \mathrm{D} \Rightarrow & \left[\left(\frac{m-1}{4}\right)^3 + 3\left(\frac{m-1}{4}\right)^2 + 3\left(\frac{m-1}{4}\right) + 1\right]\Delta \\ & = \left[\left(\frac{m-1}{4}\right) + 1\right]^3. \end{aligned} \tag{6}$$

The maximum number of delays is obtained by visiting each mirror $[(m - 1)/4]$ times, or

$$\begin{aligned} N_{\mathrm{quartic}} &= \left\{\begin{aligned} &\left(\frac{m}{4}\right)\left[\left(\frac{m-1}{4}\right)^3 + 3\left(\frac{m-1}{4}\right)^2 + 3\left(\frac{m-1}{4}\right) + 1\right] + \\ &\left(\frac{m-1}{4}\right)\left[\left(\frac{m-1}{4}\right)^2 + 2\left(\frac{m-1}{4}\right) + 1\right] + \\ &\left(\frac{m-1}{4}\right)\left[\left(\frac{m-1}{4}\right) + 1\right] + \\ &\left(\frac{m-1}{4}\right)[1] \end{aligned}\right\} \\ &= \left[\left(\frac{m-1}{4}\right)^4 + 4\left(\frac{m-1}{4}\right)^3 + 6\left(\frac{m-1}{4}\right)^2 + 4\left(\frac{m-1}{4}\right)\right] \\ &= \left[\left(\frac{m-1}{4}\right) + 1\right]^4 - 1. \end{aligned} \tag{7}$$

Table 1. Mirror Progressions in the Quartic Cell[a]

Delay	Mirror Progression
0Δ	AB AB AB AB A BA BA BA BA
1Δ	AB AB AB AB A BA BA BA CA
2Δ	AB AB AB AB A BA BA CA CA
3Δ	AB AB AB AB A BA CA CA CA
4Δ	AB AB AB AB A CA CA CA CA
5Δ (first use of E)	AB AB AB AB A BA BA BA BE
6Δ (5 + 1)	AB AB AB AB A BA BA BA CE
7Δ (5 + 2)	AB AB AB AB A BA BA CA CE
8Δ (5 + 3)	AB AB AB AB A BA CA CA CE
9Δ (5 + 4)	AB AB AB AB A CA CA CA CE
10 (two visits to E)	AB AB AB AB A BA BA BE BE
11Δ (10 + 1)	AB AB AB AB A BA BA BE CE
⋮	
24Δ (4 visits to E and to C)	AB AB AB AB A CE CE CE CE
25Δ (first visit to F)	AF AB AB AB A BA BA BA BA
⋮	
124Δ (4 visits to C, E, and F)	AF AF AF AF A CE CE CE CE
125Δ (first use of D)	DB AB AB AB A BA BA BA BA
126Δ (100 + 1)	DB AB AB AB A BA BA BA CA
⋮	
500Δ	DB DB DB DB A BA BA BA BA
⋮	
619Δ (3 visits to E, 4 visits to D, F, C)	DF DF DF DF A CE CE CE CA
624Δ	DF DF DF DF A CE CE CE CE

[a]With one transitional bounce (the 9th bounce, to mirror A), for $m = 17$ bounces and a maximum delay of 624Δ.

This equation is quartic in $(m - 1)/4$, and we call this device the quartic cell. From Eq. (7), is $m = 17$, the number of delays obtainable is $N_{\text{quartic}} = 624$. Each delay mirror is visited up to $[(m - 1)/4] = 4$ times. Table 1 shows the progression of mirrors for some selected delays in the quartic cell. Note that in every case we transfer from one loop to the other with a visit to A after the 8th bounce. We call this extra bounce a transitional bounce. In the next section, we show an alternate design that eliminates this extra bounce at the cost of one delay.

B. Design Eliminating Transitional Bounce

In practice, however, we should do everything possible to reduce the number of bounces. Each bounce in the White cell will increase the loss, increase the required tolerance on alignment, and compound any aberrations such as astigmatism. It turns out that the only time we absolutely need the transitional bounce to A describe in Subsection 3.A is when every delay mirror is traveled to every time (the last delay in the table). We can, however, obtain every delay up to this one by careful rearrangement of the order in which the mirrors are traveled to, and eliminate the extra bounce. This is shown in Table 2 for $m = 16$. For example, approximately for the first 100 or more delays, we arbitarily traveled to the ACEB loop during the last bounces, but at delay 124 we needed to go to this loop first, to make sure that there was an opportunity to go through A to get to F.

For the last delay, we cannot travel to the shortest (mirror C) a fourth time because we have visited every other mirror four times and require one bounce in the null cell to go from one loop to the other. It is possible, however, to travel to mirror C four times as long as some other mirror is traveled to fewer times. In other words, we can obtain every delay up to and including 623Δ. We have given up only one delay, but eliminated one round trip through the cell, a good tradeoff.

The mirror assignments for the improved quartic cell are

$$\begin{aligned}
&\mathrm{C} \Rightarrow 1\Delta \\
&\mathrm{E} \Rightarrow \left(\frac{m}{4} + 1\right)\Delta \\
&\mathrm{F} \Rightarrow \left[\left(\frac{m}{4}\right)^2 + 2\left(\frac{m}{4}\right) + 1\right]\Delta = \left[\left(\frac{m}{4}\right) + 1\right]^2\Delta \\
&\mathrm{D} \Rightarrow \left[\left(\frac{m}{4}\right)^3 + 3\left(\frac{m}{4}\right)^2 + 3\left(\frac{m}{4}\right) + 1\right]\Delta. \qquad (8)
\end{aligned}$$

And the number of delays that can be obtained is

$$\begin{aligned}
N_{\text{improved quartic}} &= \left[\left(\frac{m}{4}\right)^3 + 4\left(\frac{m}{4}\right)^3 + 6\left(\frac{m}{4}\right)^2 \right. \\
&\quad \left. + 4\left(\frac{m}{4}\right) - 1\right] \\
&= \left[\left(\frac{m}{4}\right) + 1\right]^4 - 2. \qquad (9)
\end{aligned}$$

Table 2. Some Mirror Progressions for the Improved Quartic Cell[a]

Delay	Mirror Progression
0Δ	AB AB AB AB AB AB AB AB
1Δ	AB AB AB AB AB AB AB AC
2Δ	AB AB AB AB AB AB AC AC
3Δ	AB AB AB AB AB AC AC AC
4Δ	AB AB AB AB AC AC AC AC
5Δ (first use of E)	AB AB AB AB AB AB AB EB
6Δ (5 + 1	AB AB AB AB AB AB AB EC
7Δ (5 + 2)	AB AB AB AB AB AB AC EC
8Δ (5 + 3)	AB AB AB AB AB AC AC EC
9Δ (5 + 4)	AB AB AB AB AC AC AC EC
10 (two visits to E)	AB AB AB AB AB AB EB EB
11Δ (10 + 1)	AB AB AB AB AB AB EB EC
⋮	
24Δ (4 visits to E and to C)	AB AB AB AB EC EC EC EC
25Δ (first visit to F)	AF AB AB AB AB AB AB AB
⋮	
124Δ (4 visits to C, E, and F) (note order reversal)	EC EC EC EC AF AF AF AF
125Δ (first use of D)	DB AB AB AB AB AB AB AB
126Δ (100 + 1)	DB AB AB AB AB AB AB AC
⋮	
499Δ (3 visits to D plus 124Δ as above)	EC EC EC EC AF DF DF DF
500Δ	DB DB DB DB AB AB AB AB
⋮	
523Δ (500 + 5 + 5 + 5 + 5 + 1 + 1 + 1)	DB DB DB DB EB EC EC EC
524Δ	DB DB DB DB EC EC EC EC
599Δ (3 times to F, 4 times to D, plus 24)	DF DF DF DB EC EC EC EC
600Δ (4 times to F and to D)	DF DF DF DF AB AB AB AB
604Δ (600 + 4)	DF DF DF DF AC AC AC AC
619Δ (3 visits to E, 4 visits to D, F, C)	DF DF DF DF AC EC EC EC
620Δ (4 times to E plus 600)	EB EB EB EB DF DF DF DF
621Δ (620 + 1)	EC EB EB EB DF DF DF DF
622Δ (620 + 2)	EC EC EB EB DF DF DF DF
623Δ (620 + 3) (max delay)	EC EC EC EB DF DF DF DF
(624Δ) (prohibited)	(DF DF DF D[F C]E CE CE CE) or (CE CE CE C[E D]F DF DF DF DF)[b]

[a]With no transitional bounce, for $m = 16$. One delay fewer can be obtained compared with Table 1, but with one less bounce.
[b]Boxes highlight prohibited progressions.

In simplifying these expressions [Eqs. (4), (6), (7), and (9)], we have noted that the coefficients of each term are those of Pascal's triangle.

In the next section we extrapolate these results to higher-order polynomial TTD cells.

4. Higher-Order Cells

One could continue this process if one had access to MEM mirror arrays with even more stable states. For each additional state, two more White (spherical) mirrors can be added, increasing the order of the polynomial cell by two. For example, a MEM whose pixels can tip to five different positions could produce an octic cell using ten spherical mirrors. Here we will present two different designs for octic cells, based on two different styles of five-state tip-tilt micro-mirror arrays.

A. Flower-Petal Design Based on Two Quartic Cells with One Transitional Bounce between Them

Let us assume first a MEM whose pixels can tip to five stable positions, and let those positions be flat, and tipped θ° in each of the East, West, North, and South directions. A TTD device based on this hypothetical MEM is shown in Fig. 4. We call this configuration the flower-petal design. The connectivity diagram for the flower-petal design is also shown in Fig. 4. Mirrors A and B again form a null cell: a light beam circulating only between these leaves the cell with a net delay of zero compared to the delay via alternate paths.

The octic cell may be considered to be composed of two quartic cells, one in the East–West plane and the other in the North–South plane. We use two quartic cells of the type that do not use transitional bounces (Subsection 3.B). We assign Mirrors C, E, D, and F, in the East–West quartic cell, as in Eq. (8), with two modifications. First, we need to share the total number of bounces among all White-cell mirrors. In the quartic cell there were four mirrors excluding the null cell; here there are eight mirrors that contribute to the time delay. Therefore the basic increment in Eq. (6) becomes $m/8$, where the

denominator reflects the number of delay-bearing White-cell mirrors.

Second, we enable one transitional bounce to switch from the East–West quartic cell to the North–South one. Thus our counting basis is $(m-1)/8$, and m is again an odd number.

The mirror assignments for the East–West quartic cell are [compare to Eq. (8)]

$$\mathrm{C} \Rightarrow 1\Delta$$

$$\mathrm{E} \Rightarrow \left(\frac{m-1}{8}+1\right)\Delta$$

$$\mathrm{D} \Rightarrow \left[\left(\frac{m-1}{8}\right)^2+2\left(\frac{m-1}{8}\right)+1\right]\Delta = \left[\left(\frac{m-1}{8}\right)+1\right]^2\Delta$$

$$\mathrm{F} \Rightarrow \left[\left(\frac{m-1}{8}\right)^3+3\left(\frac{m-1}{8}\right)^2+3\left(\frac{m-1}{8}\right)^1+1\right]\Delta = \left[\left(\frac{m-1}{4}\right)+1\right]^3\Delta. \quad (10)$$

From Eq. (9), we know that the maximum delay obtainable using just these mirrors will be

$$N_{\mathrm{CEDF}} = \left[\left(\frac{m-1}{8}\right)^4+4\left(\frac{m-1}{8}\right)^3+6\left(\frac{m-1}{8}\right)^2+4\left(\frac{m-1}{8}\right)-1\right] = \left[\left(\frac{m-1}{8}\right)+1\right]^4-2.$$

Thus we make the longest arm, say G, longer than this by one increment:

$$\mathrm{G} \Rightarrow \left[\left(\frac{m-1}{8}\right)^4+4\left(\frac{m-1}{8}\right)^3+6\left(\frac{m-1}{8}\right)^2+4\left(\frac{m-1}{8}\right)\right]\Delta. \quad (11)$$

The maximum delay obtainable using just C, E, D, F,and G is given by Eq. (9) plus $m/8$ visits to G:

$$N_{\mathrm{CEDFG}} = \left(\frac{m-1}{8}\right)\left[\left(\frac{m-1}{8}\right)^4+4\left(\frac{m-1}{8}\right)^3+6\left(\frac{m-1}{8}\right)^2+4\left(\frac{m-1}{8}\right)\right]+\left[\left(\frac{m-1}{8}\right)^4+4\left(\frac{m-1}{8}\right)^3+6\left(\frac{m-1}{8}\right)^2+4\left(\frac{m-1}{8}\right)-1\right] = \left[\left(\frac{m-1}{8}\right)^5+5\left(\frac{m-1}{8}\right)^4+10\left(\frac{m-1}{8}\right)^3+10\left(\frac{m-1}{8}\right)^2+4\left(\frac{m-1}{8}\right)-1\right]. \quad (12)$$

The next arm is one greater than this, etc. The remaining assignments are

$$\mathrm{J} \Rightarrow \left[\left(\frac{m-1}{8}\right)^5+5\left(\frac{m-1}{8}\right)^4+10\left(\frac{m-1}{8}\right)^3+10\left(\frac{m-1}{8}\right)^2+4\left(\frac{m-1}{8}\right)\right]\Delta$$

$$\mathrm{H} \Rightarrow \left[\left(\frac{m-1}{8}\right)^6+6\left(\frac{m-1}{8}\right)^5+15\left(\frac{m-1}{8}\right)^4+20\left(\frac{m-1}{8}\right)^3+14\left(\frac{m-1}{8}\right)^2+4\left(\frac{m-1}{8}\right)\right]\Delta$$

$$\mathrm{K} \Rightarrow \left[\left(\frac{m-1}{8}\right)^7+7\left(\frac{m-1}{8}\right)^6+21\left(\frac{m-1}{8}\right)^5+35\left(\frac{m-1}{8}\right)^4+34\left(\frac{m-1}{8}\right)^3+18\left(\frac{m-1}{8}\right)^2+4\left(\frac{m-1}{8}\right)\right]\Delta. \quad (13)$$

Note that now the coefficients no longer follow Pascal's triangle.

The maximum number of unique delays that can be produced would be obtained by traveling to each of the eight delay mirrors as many times as possible. Recall that in the improved quartic cell (no transitional bounce), one could travel to three of the four delay mirrors $m/4$ times, but travel to the shortest mirror one time less, to allow a bounce in the null cell to transition from one loop to another. This happens again here in the East–West plane. Because the octic cell can be thought of as two conjoined quartic cells, it will also be true that in the N–S octic cell, one can travel to three of the mirrors $(m-1)/8$ times but the other one a time fewer. To obtain the highest number of different delays, we choose the shortest mirror in the North–South plane to skip (G). Thus the total number of delays obtainable in this device would involve $(m-1)/8$ trips to mirrors D, E, and F in the East–West quartic cell and mirrors J, H, and K

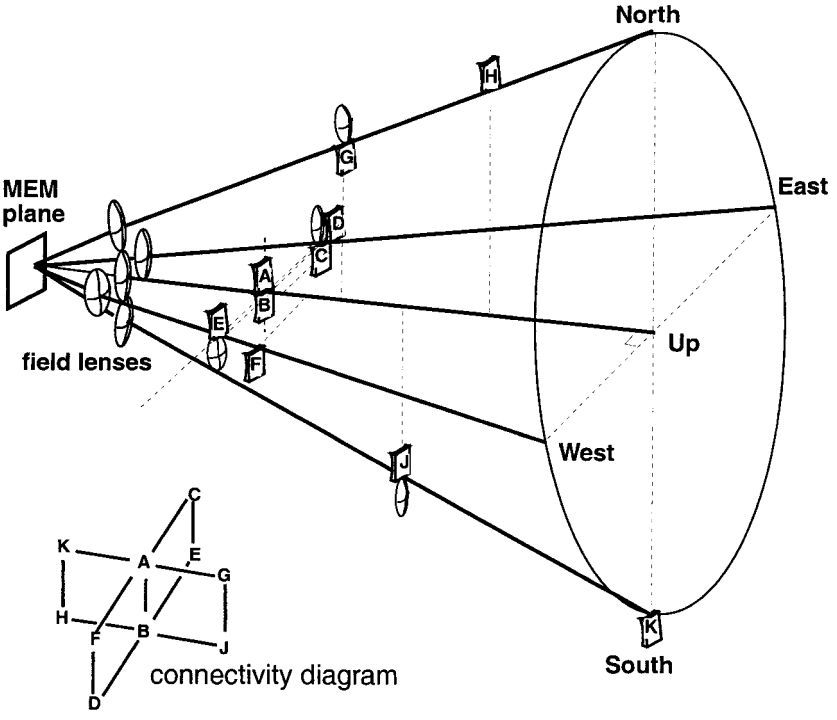

Fig. 4. Flower-petal octic TTD cell is based on a MEM with five stable micromirror tip angles: flat, and θ degrees to East, West, North, and South.

in the North–South quartic cell, and $[(m-1)/8]-1$ trips to C in the East–West cell and G in the North–South cell. The total number of delays obtainable with this design can be shown to be

$$N_{\text{octic}} = \left[\left(\frac{m-1}{8}\right)^8 + 8\left(\frac{m-1}{8}\right)^7 + 28\left(\frac{m-1}{8}\right)^6 + 56\left(\frac{m-1}{8}\right)^5 + 68\left(\frac{m-1}{8}\right)^4 + 48\left(\frac{m-1}{8}\right)^3 + 16\left(\frac{m-1}{8}\right)^2 + 0\left(\frac{m-1}{8}\right) - 1\right]. \quad (14)$$

Here we are counting in a base-$(m-1)/8$ system.

For a 17-bounce system, $(m-1)/8 = 2$, and this cell is octic in 2. The total number of delays is 6399, approximately a 10-fold improvement over the quartic cell with a comparable number of bounces.

The mirror progressions for some selected delays are shown in Table 3 for a flower-petal octic cell with one transitional bounce, with $m = 17$. The mirror assignments are C = 1Δ, E = 3Δ, D = 9Δ, F = 27Δ, G = 80Δ, J = 240Δ, H = 720Δ and K = 2160Δ.

B. Flower-Petal Design with Extra Transitional Bounces

In developing the cell of Subsection 4.A, we used two strategies. In each quartic arm, we traveled to one mirror one time fewer than the others to enable one bounce in the null cell to allow a transition from one loop to the other. We gave up one trip to mirror C (delay of 1Δ) and one trip to mirror G (a delay of 80Δ for $m = 17$). It is not of great significance to give up one delay in exchange for one bounce, but we might be more reluctant to give up 80 delays. Thus we can modify the design of Subsection 4.A so that the quartic cell in the East–West plane has no transitional bounce (giving up a delay of 1Δ), but the North–West cell has a transitional bounce, to allow all possible trips to all delay arms. Also, we enable one transitional bounce to go from the East–West plane to the North–South plane. This would result in a cell octic in $(m-2)/8$. If this strategy is chosen, then the coefficients for the term in each of the delays chosen for each delay arm would, in fact, follow Pascal's triangle, and the number of delays obtainable would be

$$N_{\text{alternate flower–petal}} = \left[\left(\frac{m-2}{8}\right)^8 + 8\left(\frac{m-2}{8}\right)^7 + 28\left(\frac{m-2}{8}\right)^6 + 56\left(\frac{m-2}{8}\right)^5 + 70\left(\frac{m-2}{8}\right)^4 + 56\left(\frac{m-2}{8}\right)^3 + 28\left(\frac{m-2}{8}\right)^2 + 8\left(\frac{m-2}{8}\right) - 1\right]$$
$$= \left[\left(\frac{m-2}{8}\right) + 1\right]^8 - 2. \quad (15)$$

Table 3. Some Mirror Progressions in the Flower-Petal Octic Cell[a]

Delay	Mirror Progression
0Δ	AB AB AB AB A BA BA BA BA
1Δ	AB AB AB AB A BA BA BA CA
2Δ	AB AB AB AB A BA BA CA CA
3Δ (first use of E = 3)	AB AB AB AB A BA BA BA BE
8Δ (two visits each to C, E)	AB AB AB AB A BA BA CE CE
9Δ (first use of D = 9)	AB AB AB AB A BA BD BA BA
26Δ (max number of times to C, D, E)	AB AB AB AB A CE CE BD BD
27Δ (first use of F = 27)	AB AB AB AB A BA FB AB AB
79Δ (max use of C, D, E, F)	AB AB AB AB A FD FD CE CE
80Δ (first use of G = 80)	AB AB AB AG A BA BA BA BA
239 (max use of C, D, E, F, G)	AB AB AG AG A FD FD BE CE
240Δ (first use of J = 240)	AB AB AB JB A BA BA BA BA
719Δ (max use of C, D, E, F, G, J), (79 + twice to G and J)	AB AB JG JG A FD FD BE CE
720Δ (first use of H = 720)	AB AB AB HB A BA BA BA BA
1000Δ	AB AB HB JB A FD AB CE AB
2159Δ (max use of C, D, E, F, G, J, H)	HB HB JG JG A FD BE CE
2160Δ (max use of C, D, E, F, G, J, H)	HB HB JG JG A FD FD BE CE
2160Δ (first use of K = 2160)	AK AB AB AB A BA BA BA BA
6399 (max delay)	JG JB HK HK A FD FD BE CE

[a]With $m = 17$ and one transitional bounce.

Table 4 shows the key delays with this alternate approach. The assignments are C = 1Δ, E = 3Δ, F = 9Δ, G − 27Δ, G = 81Δ, J = 243Δ, H = 729Δ, and K = 2187Δ.

It might appear as though the alternate design (Table 4) is slightly better, because it produces more delays (6550 delays in 18 bounces), compared to the 6399 delays in a comparable 17 bounces. In practice, however, it is unlikely to make much difference whether one has 6550 or 6399 delays (a 4% change). The losses in the White cell will, however, accumulate on each bounce, so there is motivation to minimize the number of bounces. Also, fewer bounces mean fewer pixels required on the MEM, and also may ease alignment tolerances somewhat. Furthermore, the lengths of the arms required in the alternate design are slightly larger, increasing the overall size of the device. There is a much stronger motivation than all of these, however. In Subsection 4.D, we show that the MEM can be greatly simplified using the design of Subsection 4.A (one transitional bounce) compared with the design of Subsection 4.B (two transitional bounces). Thus the design that uses a single transitional bounce is preferable in most circumstances.

Next we develop another octic cell based on a different style of MEM.

C. Broom Design

Another way of building a 5-state MEM could be imagined, in which the five positions of tiler are all in one plane. Suppose the positions are flat, $\pm\theta$, and

Table 4. Some Mirror Progressions for the Alternatie Flower-Petal Design[a]

Delay	Mirror Progression
0Δ	AB AB AB AB AB AB AB AB AB
1Δ (first use of C = 1)	AB AB AB AB AB AB AB AB AC
2Δ	AB AB AB AB AB AB AB AC AC
3Δ (first use of E = 3)	AB AB AB AB AB AB AB AB EB
8Δ (two visits each to C, E)	AB AB AB AB AB AB AB EC EC
9Δ (first use of D = 9)	AB AB AB AB AB DB AB AB AB
26Δ (max number of times to D, F, E)	AB AB AB AB DB DB EC EC
27Δ (first use of F = 27)	AB AB AB AB AF AB AB AB AB
80Δ (max use of C, E, D, F)	AB AB AB AB DB DB AB EC EC
81Δ (first use of G = 81)	AB AB AB AG AB AB AB AB AB
242 (max use of C, E, D, F, G)	AB AB AG AG AC EC EB DF DF
243Δ (first use of J = 243)	AB AB JB AB AB AB AB AB AB
728Δ (max use of C, E, D, F, G, J)	AB AB JG JG AC EC EB DF DF
729Δ (first use of H = 729	HB AB AB AB AB AB AB AB AB
2186Δ (max use of C, E, D, F, G, J, H)	HB HB JG JG AC EC AB DF DF
2187Δ (first use of K = 2187)	AK AB AB AB AB AB AB AB AB
6559 (max delay)	HK HK AF DF DB EC EB JG JG

[a]With $m = 18$ and two transitional bounces.

$\pm 2\theta$. Figure 5 shows how the ten White-cell mirrors could be arranged, splaying out like the straws of a broom.

In this arrangement, the connectivity diagram is modified. When a pixel is flat, beams can go from A to B, C to E, D to F, G to J, and H to K. A beam can go directly from D to K if the pixel is tipped to $-\theta$, a connection that was not possible in the flower-petal design. The complete connectivity diagram for the broom design is shown in the figure. It can be seen that a much larger number of connections is possible compared with the flower-petal arrangement, and thus the choices of arms lengths will be different, and more delays can be produced for a given number of bounces than in any of the previous designs.

We still count bounces in groups of eight ($m/8$), but now the assignments are

$$\begin{aligned}
\mathrm{C} &\Rightarrow 1\Delta, \\
\mathrm{D} &= \left(\frac{m}{8} + 1\right)\Delta, \\
\mathrm{E} &= \left(\frac{m}{8} + 1\right)^2\Delta, \\
\mathrm{F} &= \left(\frac{m}{8} + 1\right)^3\Delta, \\
\mathrm{G} &= \left(\frac{m}{8} + 1\right)^4\Delta, \\
\mathrm{H} &= \left(\frac{m}{8} + 1\right)^5\Delta, \\
\mathrm{J} &= \left(\frac{m}{8} + 1\right)^6\Delta, \\
\mathrm{K} &= \left(\frac{m}{8} + 1\right)^7\Delta, \qquad (16)
\end{aligned}$$

The maximum number of delays that can be produced with the broom design is

$$N_{\mathrm{octic,broom}} = \left(\frac{m}{8} + 1\right)^8. \qquad (17)$$

The maximum delay in 16 bounces with this design is 6561, compared to 6339 in 17 bounces for the first flower-petal design. Thus the broom design produces essentially the same number of delays in two less bounces.

D. Simplifying the Microelectromechanical Mirror Arrays

By using a MEM having five states instead of three, we were able to go from a quartic to an octic White-cell based polynomial-style optical TTD device. This improved the capability by an order of magnitude for 17 bounces (624 delays for the quartic cell and 6399 delays for the octic cell). Still, the increased number of states makes the fabrication of the MEM much more complicated, requiring more mechanics and more leads as well. Furthermore, the maximum tilt angle of a tip-tilt micromirror tends to be limited because of the basic planar technology used in MEM mirror arrays today. Thus a MEM whose five states lie all in one plane (as in the broom design) will have a smaller difference angle between positions, and thus between pairs of White-cell mirrors. Figure 6 shows how the light beams are diverging from their spots on the MEM pixels, for pixels at opposite ends of the MEM going in two different directions. With a small tilt angle the beams must travel much farther before they are completely separated from beams going in other directions. For example, if the spots are Gaussian with spot size 50 μm and wavelength λ = 1.3 μm, the differences in mirror-tilt angles must be at least 9.5° for the beams to separate at all (by use of a 2σ criterion). The tilt must be greater to compensate for separation of the spots on the MEM. This is especially true for a MEM whose dimension d is large, as would be the case for a MEM with a large number of pixels. Larger d increases the minimum distance x to the field lenses, which increases the overall size of the device. (Note that it does not put limits on the size of the delays chosen because the delays are the differences between various path lengths, not the lengths themselves.) Thus our desire for large MEM tilt angles, to keep the size of the apparatus tractable, can conflict with our desire for a larger number of stable pixel states.

From Table 3 for the flower-petal design, however, we observe that, for example, the last half of the bounces are always directed to the East–West loops of Fig. 4. Thus the micromirrors at the pixels associated with these bounces do not need to be able to tilt to all five positions; they must only tilt to East, flat, or West. Similarly, bounces 1–10 will only require pixels to tip to North, South, and flat. Therefore we can replace the five-state MEM pixels with three-state MEM mirrors, some with their axes of tilt running North–South, and others with their axes running East–West, as appropriate to the row in which they occur.

This technique for simplifying the MEM by orienting three-state mirrors with different axes cannot be used in the alternate flower-petal design of Table 4. That can be seen most easily in the last row of the table, where we had to alternate between North–South loops (ABHK and ABJG) and East–West loops (ABCE and ABDF) to avoid illegal transitions.

The MEM cannot be simplified for the broom design.

5. Discussion and Conclusions

We have presented several different designs for polynomial-style optical TTD devices based on tip-tilt MEM mirror arrays with various numbers of stable states. Figure 7 shows the number of delays obtainable for the various designs as a function of the number of bounces. Let us suppose our target is 1000 delays. With the simplest, two-state MEM (the line labeled quadratic in $m/4$), we could build a quadratic cell, but it would require at least 124 bounces. With a three-state MEM one can implement a quartic cell

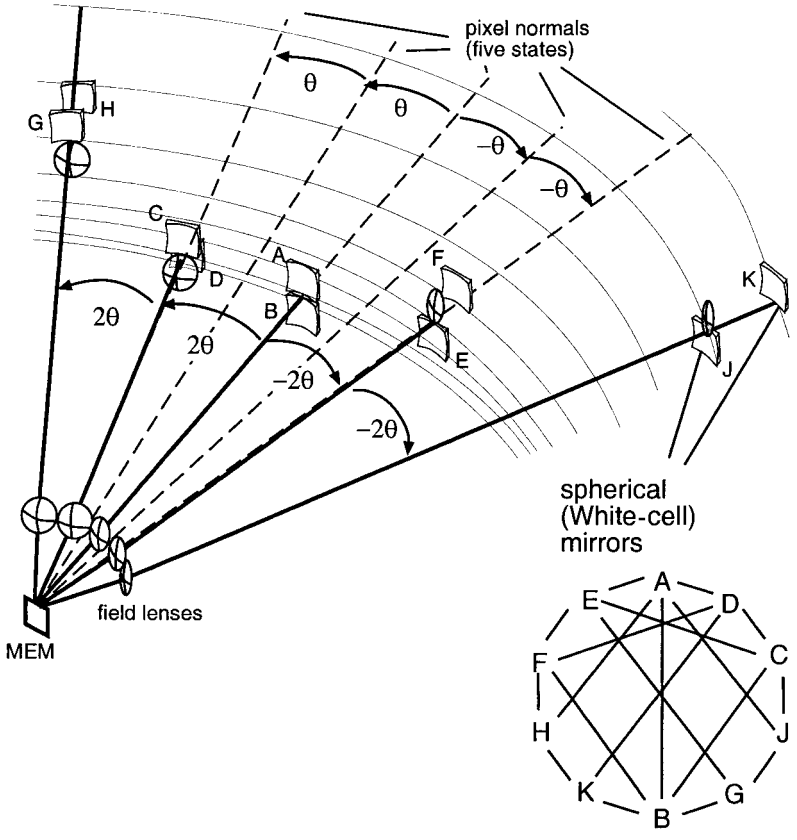

Fig. 5. Broom design for an octic cell based on a MEM with five positions: flat, $\pm\theta$, and $\pm 2\theta$, all in one plane.

and produce over 1000 delays in 20 bounces [Eq. (9)]. The $(m - 1)/8$ flower-petal design [Eq. (14)], which is octic but can be made with a three-state MEM with mirror axes at varying angles, requires 17 bounces to exceed 1000 delays.

We point out that in the octic cells, one can actually achieve 1000 delays in fewer than the number of bounces shown by designing for all the delays and then simply not using all the possible trips to the longest arm. For example, in Table 3 for the flower-petal design, even though this table is for a 17-bounce system, one need only travel to mirror H one time, and mirror K not at all to obtain a delay of 1000Δ. Therefore, the first four bounces are not used at all, and arm K does not even have to be constructed. Every delay from 0 to 1000 can be achieved in just 13 bounces. Similarly, the broom device is also octic, and it can do 1000 delays in 12 bounces if the system is designed for 16 bounces (the longest arm is again not used).

The broom octic cell [Eq. (17)] and the alternate flower-petal octic cell [Eq. (15)] require a true five-state MEM, far and away the most complex. The original flower-petal design [Eq. (14)] represents the

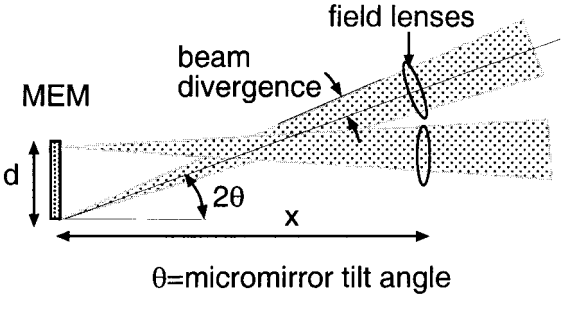

Fig. 6. The greater the pixel tip angle, the closer the field lenses can be to the MEM, and the overall size of the apparatus is reduced.

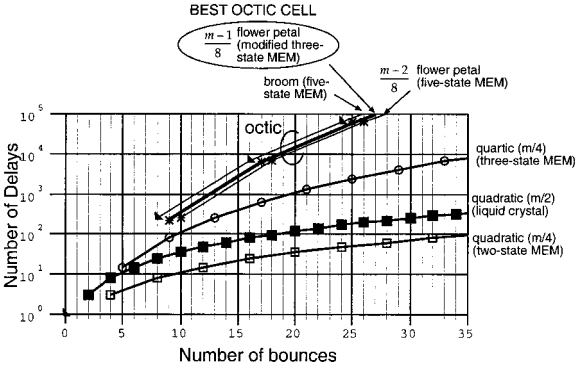

Fig. 7. Comparison of the capability of the various polynomial cells. The flower-petal design based on $(m - 1)/8$ is a good tradeoff because it produces a large number of delays but can be built with a three-state MEM.

best tradeoff between capability (number of delays) and MEM simplicity, because it can be built using a three-state MEM instead of a five-state MEM.

The ideas presented in this paper could be extended to MEM mirror arrays having even more stable states. For example, Lucent uses an analog tip-tilt micromirror array in their LambdaStar router.[29] The micromirrors of that device can tilt to an arbitrary angle within a certain cone. With access to this MEM, one could in principle add any number of White-cell arms and produce a polynomial cell of arbitrary order. In practice, however, this would not be worthwhile. As discussed in relation to Fig. 6, we require some minimum separation in angle between MEM states to avoid overlapping of beams. To have a large number of White cells (even larger than ten) would require a very large cone of possible tilt angles, which is not currently attainable given the planar nature of MEM technology. In any case, the level of complexity involved in building more than 10 White-cell arms is probably not warranted, because the octic cell of Table 3 can produce 6399 different delays in 17 bounces.

We gratefully acknowledge useful discussions with Stuart A Collins, Jr. The work in this paper extends ideas that were developed earlier and jointly with him.

References

1. H. Zmuda and E. N. Toughlian, "Photonic aspects of modern radar," in *The Artech House Optoelectronics Library*, B. Culshaw, A. Rogers, and H. Taylor, eds. (Artech House, Norwood, Mass., 1994).
2. N. Madamopoulos and N. A. Risa, "Demonstration of an all-digital 7-bit 33-channel photonic delay line for phased-array antennas," Appl. Opt. **39,** 4168–4181 (2000).
3. E. G. Paek, Y.-S. Im, J. K. Choe, and T. K. Oh, "Acoustically steered and rotated true-time delay generator based on wavelength-division multiplexing," Appl. Opt. **38,** 1298–1308 (2000).
4. M. Y. Frankel and R. D. Esman, "Reconfigurable time-steered array-antenna beam former," Appl. Opt. **36,** 9261–9268 (1997).
5. D. T. K. Tong and M. C. Wu, "Transmit-receive module of multiwavelength optically controlled phase-array antennas," IEEE Photon. Technol. Lett. **10,** 1018–1019 (1998).
6. B. Tsap, Y. Chang, H. R. Fetterman, A. F. J. Levi, D. A. Cohen, and I. Newberg, "Phased-array optically controlled receiver using a serial feed," IEEE Photon. Technol. Lett. **10,** 267–269 (1998).
7. R. L. Q. Li, X. Fu, and R. Chen, "High packing density 2.5 THz truetime delay lines using spatially multiplexed substrate guided waves in conjunction with volume holograms on a single substrate," J. Lightwave Technol. **15,** 2253–2258 (1997).
8. S. Yegnanarayanan, P. D. Trinh, and B. Jalali, "Recirculating photonic filter: a wavelength-selective time delay for phased-array antennas and wavelength code-division multiple assess," Opt. Lett. **21,** 740–742 (1996).
9. D. Dolfi and P. Joffre, "Experimental demonstration of a phased-array antenna optically controlled with phase and time delays," Appl. Opt. **8,** 1824–1828 (1996).
10. K. P. Jackson, S. A. Newton, B. Moslehi, M. Tur, C. C. Cutler, J. W. Goodman, and H. J. Shaw, "Optical fiber delay-line signal processing," IEEE Trans. Microwave Theory Tech. **MTT-33,** 193–209 (1985).
11. K.-I. Kitayama, "Code division multiplexing lightwave networks based on optical code conversion," IEEE J. Sel. Areas Commun. **16,** 1309–1319 (1998).
12. M. Tur, J. W. Goodman, B. Moslehi, J. E. Bowers, and H. J. Shaw, "Fiber-optic signal processor with applications to matrix-vector multiplication and lattice filtering," Opt. Lett. **7,** 463–465 (1982).
13. B. Moslehi, J. W. Goodman, M. Tur, and H. J. Shaw, "Fiber-optic lattice signal processing," Proc. IEEE **72,** 909–932 (1984).
14. B. Moslehi and J. W. Goodman, "Novel amplified fiber optic recirculating delay line processor," J. Lightwave Technol. **10,** 1142–1146 (1992).
15. S. Sales, J. Campany, J. MArti, and D. Pastor, "Experimental demonstration of fibre-optic delay line filters with negative coefficients," Electron. Lett. **31,** 1095–1096 (1995).
16. G. W. Euliss and R. A. Athale, "Time-integrating correlator based on fiber-optic delay lines," Opt. Lett. **19,** 649–651 (1994).
17. N. Wada, H. Sotobayshi, and K. Kitayama, "Error-free 100 km transmission at 10 GBit/s in optical code division multiplexing system using BPSK picosecond-pulse code sequence with novel time-gating detection," Electron. Lett. **35,** 833–834 (1999).
18. B. L. Anderson, J. Stuart, A. Collins, C. A. Klein, E. A. Beecher, and S. B. Brown, "Photonically produce true-time delays for phased antenna arrays," Appl. Opt. **36,** 8493–9503 (1997).
19. B. L. Anderson and C. D. Liddle, "Optical true-time delay for phased array antennas: demonstration of a quadratic White cell," to be published in Appl. Opt. **23,** 2002.
20. A. P. Goutzoulis, D. K. Davies, and J. M. Zomp, "Hybrid electronic fiber optical wavelength-multiplexed system for true time-delay steering of phased array antennas," Opt. Eng. **31,** 2312–2322 (1992).
21. H. R. Fetterman, Y. Chang, D. C. Scott, S. R. Forrest, F. M. Espiau, M. Wu, D. V. Plant, J. R. Kelly, A. Mather, W. H. Steier, and G. J. Simonis, "Optically controlled phased array radar receiver using SLM switched real time delays," IEEE Microwave Guid. Wave Lett. **5,** 414–416 (1995).
22. W. Ng and A. A. Watson, "The first demonstration of an optically steered microwave phased array antenna using true-time-delay," IEEE J. Lightwave Technol. **8,** 1124–1131 (1991).
23. P. M. Freitag and S. M. Forrest, "A coherent optically controlled phased array antenna system," IEEE Microwave Guid Wave Lett. **3,** 293–295 (1993).
24. A. P. Goutzoulis and D. K. Davies, "Hardware-compressive 2-D fiber optic delay line architecture for time steering of phased-array antennas," Appl. Opt. **29,** 5353–5359 (1990).
25. J. Stuart, A. Collins, B. L. Anderson, and C. D. Liddle, "Optical delay unit for signal processing in phased array antennas," presented at Optical Society of America Annual Meeting, Providence, Rhode Island, 2000.
26. J. White, "Long optical paths of large aperture," J. Opt. Soc. Am. **32,** 285–288 (1942).
27. B. L. Anderson, J. Stuart, A. Collins, C. A. Klein, E. A. Beecher, and S. B. Brown, "Optically Produced True-Time Delays for Phased Antenna Arrays," Appl. Opt. **36,** 8493–8503 (1997).
28. O. B. Spahn, E. J. Garcia, V. Easch, G. Grossetete, F. Bitsie, S. Mani, and J. Jakubsczak, "Optical performance of pivoting micromirrors," presented at SPIE Micromachining and Microfabrication Symposium, San Francisco, 2001.
29. D. J. Bishop, C. R. Giles, and S. R. Das, "The rise of optical switching," in Sci. Am. January, 2001, 88–94.